Origin of the different color of ruby and emerald

J. M. García-Lastra,[1] M. T. Barriuso,[1] J. A. Aramburu,[2] and M. Moreno[2]
[1]*Departamento de Física Moderna, Universidad de Cantabria, 39005 Santander, Spain*
[2]*Departamento de Ciencias de la Tierra y Física de la Materia Condensada, Universidad de Cantabria, 39005 Santander, Spain*
(Received 26 April 2005; revised manuscript received 10 June 2005; published 7 September 2005)

The different color exhibited by ruby and emerald is a fundamental but still unsolved question. According to recent EXAFS measurements, such a difference can hardly be explained on the basis of a different average distance between Cr^{3+} and the six oxygen ligands. The puzzling difference in color between the two gemstones is shown in this work to arise essentially from the distinct electrostatic potential imposed by the rest of lattice ions upon the active electrons of the CrO_6^{9-} unit. Main effects are shown to come from the electric field generated in the neighborhood of the Cr^{3+} site in ruby which is absent in the case of emerald due to symmetry.

DOI: 10.1103/PhysRevB.72.113104 PACS number(s): 71.55.−i, 71.15.Mb, 61.72.Ji, 91.60.Mk

The origin of the different color exhibited by ruby ($Al_2O_3:Cr^{3+}$) and emerald ($Be_3Si_6Al_2O_{18}:Cr^{3+}$) is a relevant but still unsolved problem.[1–11] This work aims to show that the electrostatic potential, $V_R(\mathbf{r})$, imposed by the rest of lattice ions on the active electrons of the CrO_6^{9-} complex plays a key role for understanding such a subtle difference. The influence of $V_R(\mathbf{r})$ on optical properties of gemstones has not been considered in previous studies.[1–3,7,9,11]

The impurity responsible for the color in ruby and emerald is the same, and in both gemstones Cr^{3+} is surrounded by six oxygen ligands. Nevertheless, the maximum of the $^4A_{2g} \rightarrow {}^4T_{2g}$ broad absorption band of the CrO_6^{9-} complexes appears at 18 070 cm^{-1} and 16 130 cm^{-1} for ruby and emerald, respectively.[3–5,7–9,11] Therefore, this first spin allowed transition is responsible for the characteristic red and green color of ruby and emerald, respectively. Within the framework of the ligand field theory the energy of the center of gravity of the $^4A_{2g} \rightarrow {}^4T_{2g}$ transition is just equal[12] to the cubic field splitting parameter, $10Dq$. For transition metal (TM) impurities in cubic symmetry the separation, $10Dq$, between the $e_g(\sim 3z^2-r^2, x^2-y^2)$ and $t_{2g}(\sim xy, xz, yz)$ levels is strongly sensitive to variations in the impurity-ligand distance, R. Writing $10Dq=KR^{-n}$, the exponent n is found to lie typically between 4 and 6 for TM impurities in octahedral coordination.[13–15] Microscopically, this strong R dependence of $10Dq$ has been shown to arise mainly from the small s-p hybridization on ligands involved in the e_g orbital.[16,13] Bearing in mind this sensitivity of $10Dq$ to R variations, it was first assumed by Orgel[1] that the different colors of ruby and emerald should be associated with different values of the average distance, R, between the impurity and six oxygen ligands.

According to Orgel's view, the small but relevant difference $\Delta 10Dq=1940$ cm^{-1} between ruby and emerald should then correspond to $R(\text{emerald})-R(\text{ruby})=0.05$ Å, taking $n=4.5$.[14] This interpretation thus implies the existence of a small compression of the oxygen octahedron in ruby in comparison to emerald. Although such an explanation has been considered as reasonable,[1,9] recent extended x-ray absorption fine structure (EXAFS) measurements performed on both gemstones[10,11] cast serious doubts on it. In the case of emerald, the six ligand ions are all found to be at the same distance from Cr^{3+}[R(emerald)=1.97 Å] although the ligand octahedron is slightly trigonally distorted involving a D_3 local symmetry.[11] For $Al_2O_3:Cr^{3+}$ the local symmetry is found to be C_3 with three oxygen ions placed at $R_s=1.92$ Å while the three other ligands are at $R_l=2.02$ Å.[10,11] Therefore, the average distance R(ruby)=1.97 Å coincides with that for emerald within the experimental uncertainty (±0.01 Å) involved in the EXAFS measurements.[11] It should be remarked that the energy, E_c, of the center of gravity of sharp emission lines in ruby ($E_c=14\,420$ cm^{-1})[8,17] is *only* about 1.8% *smaller* than that for emerald ($E_c=14\,690$ cm^{-1}).[4,8] The energy of the sharp $^2E_g(t_{2g}{}^3) \rightarrow {}^4A_{2g}(t_{2g}{}^3)$ transition depends on the Racah parameters B and C[12] which increase with the ionicity of the bonding between Cr^{3+} and oxygen ligands.[18,19] Thus, the higher $10Dq$ value of ruby can hardly be ascribed to a smaller covalency in this gemstone in comparison to emerald as it has been previously suggested.[7,11] This situation is certainly puzzling because available spectroscopic data and theoretical calculations on $Al_2O_3:Cr^{3+}$ indicate[14,20,21] that similarly to what is found for TM impurities in insulating materials the active electrons are *localized* in the CrO_6^{9-} complex.[12,13]

It is worthwhile to recall that electronic properties due to an impurity, M, in a cubic insulating lattice can essentially be understood just considering the MX_N complex formed with the N nearest anions. This important idea, put forward in the pioneering work by Sugano and Shulman,[22] has been verified to be right in subsequent works on TM impurities in insulators. In fact, the d-d and charge transfer transitions associated with a TM impurity in a cubic lattice have reasonably been understood considering only the MX_N complex at the experimental equilibrium distance.[23,13]

However, in ionic materials there are long-range electric fields acting on the active electrons localized within the MX_N complex which cannot in general be neglected.[24] Let us call $V_R(\mathbf{r})$ to the electrostatic potential on the complex due to all ions of the lattice not included in the MX_N unit. This kind of Madelung potential is usually neglected for explaining the optical properties of TM impurities in high symmetry lattices since it is practically constant in the complex region.[25,13] However, when the impurity site presents a lower symmetry the nonflatness exhibited by $V_R(\mathbf{r})$ has been shown to play a

relevant role.[25–27,13] In particular, an insight into the differences exhibited by the same TM complex embedded in two lattices which are not isomorphous requires one to take into account the effects of $V_R(\mathbf{r})$.[25,27]

Searching to explain the puzzling difference in color displayed by ruby and emerald, the effect of the corresponding $V_R(\mathbf{r})$ potential on the properties of the CrO_6^{9-} unit has been studied in detail through *ab initio* quantum mechanical calculations (not using parametrized Hamiltonians).[28] However, metal-ligand distances and angles have always been fixed at the experimental values for both gemstones.[10,11] It is worth noting that a fully *ab initio* resolution of the present problem using supercells or big clusters does not appears to be easy. In fact, the relative errors involved in current *ab initio* calculated metal-ligand distances in low symmetry lattices are at least of ±1.5% for any system. Due to the strong dependence of $10Dq$ upon R,[13–15] one cannot be sure of reproducing correctly the absolute value and sign of $\Delta 10Dq$ if distances are taken directly from *ab initio* calculations.

Calculations have been performed in the framework of the density functional theory (DFT) by means of the Amsterdam density functional (ADF) code.[29] The generalized gradient approximation (GGA) exchange-correlation energy was computed according to the Perdew-Wang-91 functional.[30] All atoms except oxygen were described through basis sets of TZP quality (triple-ζ STO plus one polarization function) given in the program data base and the core electrons ($1s$ -$3p$ for Cr and $1s$ for O) were kept frozen. Following previous works,[31] the best description for oxygen ions was obtained through the DZP basis set (double-ζ STO plus one polarization function). To ensure the reliability of main conclusions, DFT calculations with other basis sets have also been performed. As a salient feature the *main effect* introduced by $V_R(\mathbf{r})$ on $\Delta 10Dq$ is always found for every employed basis set or exchange-correlation functional. It is worth noting that calculated properties are found to be less dependent on the basis set[32,33] using DFT than traditional methods based in the Hartree-Fock description.

In a first step the $10Dq$ parameter has been calculated on an isolated CrO_6^{9-} complex. In a further step the same calculations have been carried out for both ruby and emerald but with the CrO_6^{9-} complex subject to the influence of the corresponding V_R potential. $10Dq$ has always been calculated following the average of configuration procedure given in Ref. 19. The center of gravity of the small splitting undergone by the t_{2g} orbital under the trigonal site symmetry has been taken into account when deriving $10Dq$. In particular, by means of these calculations an exponent $n=4.0$ has been found. This figure is not far from the value $n=4.5$ experimentally measured from the $10Dq$ variation of ruby under hydrostatic pressure.[14]

The electrostatic potential $V_R(\mathbf{r})$ coming from all ions of Al_2O_3 or $Be_3Si_6Al_2O_{18}$ crystals lying outside the CrO_6^{9-} unit has been calculated by means of the Ewald method, following the procedure described in Ref. 23. The nominal ionic charges were employed in these calculations since recent *ab initio* calculations performed on Al_2O_3 (Ref. 34) have demonstrated that the total charges on oxygen and aluminium ions are practically equal to $-2e$ and $+3e$ (e=proton charge),

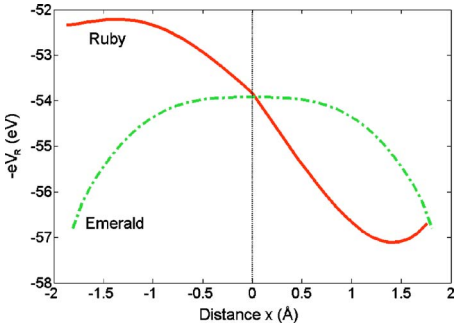

FIG. 1. (Color online) Madelung potential, $V_R(x)$, on CrO_6^{9-} along metal-ligand directions for ruby and emerald host lattices. For ruby $x>0(x<0)$ corresp onds to the long (short) bond with ligands at $R_l=2.02$ Å ($R_s=1.92$ Å) from chromium ion (Refs. 10 and 11).

respectively, pointing out that bonding is highly ionic indeed. The shape of the Madelung potential $V_R(x)$ along a metal-ligand direction (described by the x coordinate) is depicted in Fig. 1 for both gemstones.

Results of calculations are compiled in Table I. Let us call $\Delta_I 10Dq$ the $10Dq$ difference between ruby and emerald calculated for the *isolated* complex at the corresponding equilibrium geometry. By contrast the $\Delta_R 10Dq$ quantity reflects the influence of the corresponding electrostatic potential $V_R(\mathbf{r})$ upon both gemstones. When the influence of $V_R(\mathbf{r})$ is discarded the calculated $10Dq$ at the experimental distances is found to be practically the same for both systems, $\Delta_I 10Dq$ being equal to -145 cm^{-1} in Table I. However, significant changes appear when the electrostatic potential of the rest of lattice ions upon the active electrons is taken into account: $10Dq$ is found to increase by 2136 cm^{-1} in the case of ruby while in emerald it decreases but only by 449 cm^{-1}. Therefore, $\Delta_R 10Dq$ is found to be equal to 2440 cm^{-1}. This figure is thus certainly not far from the experimental value 1940 cm^{-1}. It is worth noting now that when another basis set is used a remarkable difference between $\Delta_I 10Dq$ and $\Delta_R 10Dq$ quantities is *always* obtained. For instance, if the polarization function is suppressed from the oxygen basis set, then $\Delta_I 10Dq=-207$ cm^{-1} while $\Delta_R 10Dq=2280$ cm^{-1}. On the other hand, when a TZP oxygen basis set is employed, it is found $\Delta_I 10Dq=-780$ cm^{-1} while $\Delta_R 10Dq=4700$ cm^{-1}. Furthermore the present results have been verified not to depend strongly on the actual values of charges of aluminium and oxygen ions in the host lattice. Although recent *ab initio* calculations[34] stress that Al_2O_3 is a highly ionic material (also reflected in a gap of ~9 eV) the effect of

TABLE I. Calculated values of the $10Dq$ parameter in ruby and emerald. Calculations have been performed for the CrO_6^{9-} complex *in vacuo* at experimental distances (Refs. 10 and 11) as well as including the effects of the electrostatic Madelung potential V_R on the complex. Experimental values (Refs. 7, 9, and 11) are given for comparison. Values are in cm^{-1} units.

	In vacuo	Madelung	Experimental
Ruby	16043	18179	18070
Emerald	16188	15739	16130

$V_R(\mathbf{r})$ on $10Dq$ assuming total charges on oxygen and aluminium ions equal to $-1.8e$ and $+2.7e$ respectively has also been explored. In this case it has been found that the inclusion of $V_R(\mathbf{r})$ leads to an important increase of $10Dq$ equal to 1600 cm^{-1}. All these considerations thus support that there is a *real physical effect* associated with $V_R(\mathbf{r})$ especially in the case of ruby.

The quite different effects induced by $V_R(\mathbf{r})$ on ruby and emerald can be explained by looking at $V_R(x)$ as portrayed in Fig. 1. Although the D_3 local symmetry in emerald[4,11] avoids the existence of an electric field on the electrons at the chromium site ($x=0$), the quantity $(-e)V_R(x)$ (e=proton charge) is not perfectly flat but decreases when $|x| \geq 1$ Å. This attractive potential thus decreases the energy of the t_{2g} and e_g orbitals. As σ bonding is present only in e_g, this energy lessening is found to be more pronounced for this orbital than for t_{2g}, thus leading to a reduction in $10Dq$. In the case of ruby, $V_R(x)$ looks quite different (Fig. 1) as there is an important electric field in the region $|x| \leq 1.5$ Å compatible with the lower C_3 local symmetry.[11] The polarization of the CrO_6^{9-} complex induced by this field results from the admixture of the antibonding e_g and t_{2g} orbitals with mainly $2p$ oxygen levels which are found to lie about 35 000 cm^{-1} below. This result is in agreement with the onset of charge transfer spectra of CrO_6^{9-} units.[3] The electric field associated with $V_R(x)$ in the ruby should lead to an energy decrease of mainly $2p$ oxygen levels and also to the corresponding rise of the antibonding e_g and t_{2g} levels. Therefore, this fact concurs with the result of the present DFT calculations. Such an effect produces a higher energy increase on the e_g level with σ-bonding (12 370 cm^{-1}) than on the π type t_{2g} level (10 520 cm^{-1}). Thus, this important increase in $10Dq$, which is not due to bonding in the isolated CrO_6^{9-} unit but to the action of the V_R potential on it, is the cause of the red color of ruby in comparison to emerald. We have verified that the electric field in ruby comes essentially from two Al^{3+} ions placed along the C_3 axis in the host lattice[11] but located *asymmetrically* at 2.65 Å and 3.85 Å from the Cr^{3+} position (Fig. 2).

Bearing in mind recent results on Cr^{3+}-O^{2-} distances[10,11]

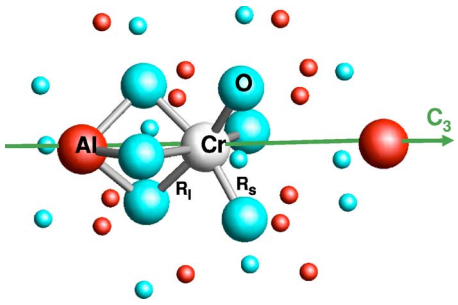

FIG. 2. (Color online) View of the first 32 neighbors around a Cr^{3+} impurity in Al_2O_3: Cr^{3+}. Ions of the CrO_6^{9-} complex as well as the two Al^{3+} ions placed asymmetrically on the C_3 axis are depicted by big balls while small balls are used for the rest of ions. The three ligands at $R_s=1.92$ Å and the Al^{3+} ion at 3.85 Å are placed to the right of Cr^{3+}.

the present arguments evidence that the difference in color between ruby and emerald is a manifestation of the electrostatic potential *imposed* by each lattice upon the CrO_6^{9-} complex. It should be emphasized that this potential, V_R, has much less importance for the emission in such gemstones since the involved states both arise from the *same* t_{2g}^3 configuration.[12] This simple reasoning thus explain why the emission line of emerald is practically coincident with that of ruby (within 1.8%) while there is a 12% difference in the energy of the $^4A_{2g} \rightarrow {}^4T_{2g}$ absorption transition.

From the present conclusions $V_R(\mathbf{r})$ can play a key role for explaining the subtle changes of color displayed by different oxides containing the same impurity.[5,7,9] In particular, the subtle changes of color obtained on passing from emerald ($Be_3Si_6Al_2O_{18}:Cr^{3+}$) to alexandrite ($BeAl_2O_4:Cr^{3+}$) or ruby spinel ($MgAl_2O_4:Cr^{3+}$) gemstones[7,9] require investigation into the influence of $V_R(\mathbf{r})$ on them. Work along this line is now under way.

The authors acknowledge the information on their EXAFS results kindly provided by Dr Ph. Sainctavit and Dr E. Gaudry and partial support by the Spanish Ministerio de Ciencia y Tecnología under Project No. BFM2002-01730.

[1] L. E. Orgel, Nature **179**, 1348 (1957).
[2] L. Singh, Nature **181**, 1264 (1958).
[3] D. S. J. McClure, J. Chem. Phys. **36**, 2757 (1962).
[4] D. L. J. Wood, J. Chem. Phys. **42**, 3404 (1965).
[5] C. P. Poole, J. Phys. Chem. Solids **25**, 1169 (1964).
[6] H. Carstens, Contrib. Mineral. Petrol. **41**, 273 (1973).
[7] K. Nassau, *The Physics and Chemistry of Colour* (John Wiley & Sons, New York, 1983).
[8] B. Canny, J. C. Chervin, D. Curie, J. Gonzalez, D. Berry, and S. A. Ho, in *Spectroscopy of Solid-State Laser-Type Materials*, (edited by B. Di Bartolo (Ettore Majorana International Science Series, Geneva, 1987), p. 431.
[9] R. G. Burns, *Mineralogical Applications of Crystal Field Theory* (Cambridge University Press, Cambridge, 1993).
[10] E. Gaudry, A. Kiratisin, P. Sainctavit, C. Brouder, F. Mauri, A. Ramos, A. Rogalev, and J. Goulon, Phys. Rev. B **67**, 094108 (2003).
[11] E. Gaudry, Ph.D. thesis, Université Paris 6, 2004.
[12] S. Sugano, Y. Tanabe, and H. Kamimura, *Multiplets of Transition-Metal Ions in Crystals* (Academic Press, New York, 1970).
[13] M. Moreno, J. A. Aramburu, and M. T. Barriuso, Struct. Bonding (Berlin) **106**, 127 (2004).
[14] S. J. Duclos, Y. K. Vohra, and A. L. Ruoff, Phys. Rev. B **41**, 5372 (1990).
[15] K. L. Bray, Top. Curr. Chem. **213**, 1 (2001).
[16] M. Moreno, J. A. Aramburu, and M. T. Barriuso, Phys. Rev. B **56**, 14423 (1997).
[17] A. H. Jahren, M. B. Kruger, and R. J. Jeanloz, J. Appl. Phys. **71**,

1579 (1992).
[18] C. K. Jørgensen, *Modern Aspects of Ligand Field Theory* (North-Holland, Amsterdam, 1971).
[19] M. Atanasov, C. A. Daul, and C. Rauzy, Chem. Phys. Lett. **367**, 737 (2003).
[20] R. W. Terhune, J. Lambe, C. Kikuchi, and J. Baker, Phys. Rev. **123**, 1265 (1961).
[21] K. Ogasawara, T. Ishii, I. Tanaka, and H. Adachi, Phys. Rev. B **61**, 143 (2000).
[22] S. Sugano and R. G. Shulman, Phys. Rev. **130**, 517 (1963).
[23] J. A. Aramburu, M. Moreno, K. Doclo, C. Daul, and M. T. Barriuso, J. Chem. Phys. **110**, 1497 (1999).
[24] W. Kohn, Phys. Rev. Lett. **76**, 3168 (1995).
[25] K. Pierloot, E. van Praet, and L. G. Vanquickenborne, J. Chem. Phys. **96**, 4163 (1992).
[26] J. A. Aramburu and M. Moreno, Phys. Rev. B **56**, 604 (1997).
[27] J. M. García-Lastra, J. A. Aramburu, M. T. Barriuso, and M. Moreno, Phys. Rev. Lett. **93**, 226402 (2004).
[28] M. Brik, N. Avram, and C. Avram, Solid State Commun. **132**, 831 (2004).
[29] G. te Velde, F. M. Bickelhaupt, E. J. Baerends, C. Fonseca Guerra, S. J. A. van Gisbergen, J. G. Snijders, and T. Ziegler, J. Comput. Chem. **22**, 931 (2001).
[30] J. P. Perdew, J. A. Chevary, S. H. Vosko, K. A. Jackson, M. R. Pederson, D. J. Singh, and C. Fiolhais, Phys. Rev. B **46**, 6671 (1992).
[31] J. A. Aramburu, J. M. García-Lastra, M. T. Barriuso, and M. Moreno, Int. J. Quantum Chem. **91**, 197 (2003).
[32] N. Lopez and F. J. Illas, J. Phys. Chem. B **102**, 1430 (1998).
[33] M. T. Barriuso, J. A. Aramburu, and M. Moreno, J. Phys.: Condens. Matter **11**, L525 (1999).
[34] C. Sousa, C. de Graaf, and F. Illas, Phys. Rev. B **62**, 10013 (2000).